Demonstration of Plasma Beat Wave Acceleration of Electrons from 2 MeV to 20 MeV

C. E. Clayton, K. A. Marsh, M. Everett, A. Lal, and C. Joshi
Department of Electrical Engineering
University of California at Los Angeles
56-125B Engineering IV
Los Angeles, CA 90024

Abstract

We describe the results from recent experiments[1] on the plasma beat wave accelerator (PBWA) scheme at UCLA. A relativistic electron plasma wave (which is the accelerating structure) is resonantly excited in a plasma by the beating of two co-propagating electromagnetic waves (obtained from a CO_2 laser operating simultaneously on two wavelengths). A 2 MeV, 200 mA (peak-current) electron beam, roughly 1 nsec (FWHM) in duration is used as a source of test particles for measuring the longitudinal fields of the plasma wave which itself is moving with a relativistic Lorentz factor of about 34. Accelerated electrons are energy-selected with an imaging sector magnet and detected simultaneously with a cloud chamber and surface barrier detectors. Initial experiments show that electrons are accelerated up to 20 MeV over roughly 1 cm (the uniform length of plasma) indicating an gradient of acceleration of more than 1.8 GeV/m.

INTRODUCTION

In the last 5 or 10 years, there has been a great deal of interest in advanced accelerator concepts.[2] The primary motivation behind this research is to increase acceleration gradients to levels beyond the ≈ 100 MeV/m limit of conventional rf technology. Much of this effort has been in the area of collective acceleration using plasmas.[3] Plasma technology has the potential for 10–100× higher gradients than state-of-the-art rf technology. For example, for a working plasma density of n_e and a plasma wave amplitude of ε, the accelerating electric field E_{accel} is given by $E_{accel} \approx \varepsilon(n_e)^{1/2}$ (eV/cm) for n_e expressed in electrons/cm^{-3}. This gives $1 < E_{accel} < 10$ GeV/m for $10^{15} < n_e < 10^{17}$ cm^{-3} and a modest wave amplitude of 30%. Potential applications of this technology are in compact GeV-scale linacs and perhaps more affordable TeV-scale linear colliders. This paper presents some recent experimental results on one such plasma accelerator concept, namely the plasma beat wave accelerator.

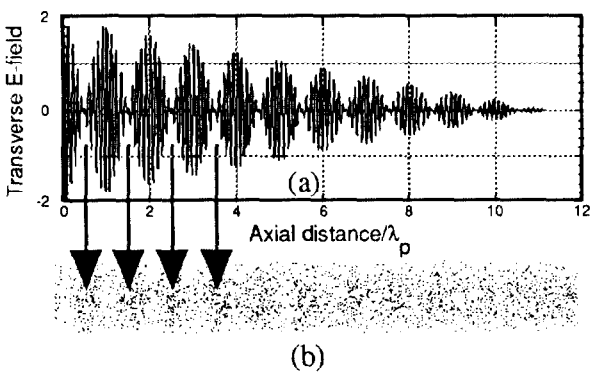

Figure 1: (a) Interference or beat pattern formed by two laser beams of slightly different frequencies. (b) Density bunching caused by the longitudinal ponderomotive force from the intensity gradients in (a).

PHYSICAL MECHANISM

The accelerator structure in the plasma beat wave scheme is an electron plasma wave which is a normal mode of the plasma. The means by which this wave is excited is illustrated in Fig. 1. When two laser beams of slightly different frequency are propagating together, there is constructive and destructive interference of their transverse electric fields forming a beat envelope as shown in Fig. 1(a). In this case, there is a longitudinal modulation to the total field intensity. The plasma electrons experience a force, called the ponderomotive force, which is proportional to the gradient of the field intensity and is thus directed towards the local minima of the beat-envelope pattern. This tends to bunch the electrons into the minima of the beat envelope (as shown in Fig. 1(b)) with a period given by the difference wavenumber Δk. As the beat envelope propagates (to the right in Fig. 1), the electrons oscillate longitudinally at the difference frequency $\Delta\omega$. Now, because the plasma ions are too massive to respond to the beating force, they do not move and so the electrons will also feel a restoring force due to the space-charge field between the bunched electrons and the still uniform ions. The plasma frequency ω_{pe} is the natural frequency of this mode of oscillation (where plasma electrons are displaced from their equilibrium position). If the plasma density and thus the plasma frequency is chosen such that $\omega_{pe} = \Delta\omega$, then the plasma wave will grow rapidly with time until a nonlinear relativistic saturation[4] limits the amplitude to $\varepsilon \approx 40\%$ (typically) for our experimental parameters.

OVERVIEW OF EXPERIMENT

A cartoon of the top-view of the experiment is shown in Fig. 2. The two-frequency laser beam[5] is focused into a vacuum chamber filled with about 140 mT of hydrogen gas. The plasma is formed by laser-ionization of the gas through tunneling ionization.[6] Upon full ionization, the plasma wave grows up and, since the bunched electrons resemble a grating, the wave can scatter optical beams, thus allowing optical diagnostics of the wave. The parameters for the laser and

plasma/plasma wave are given in Table 1. An important point to note is that the Rayleigh range is about 1 cm and this will be one of the limiting factors in the experiment. The electric fields of the wave are probed directly by injecting electrons from an electron linac.[7] The linac parameters are also summarized in Table 1. The electrons are focused through a

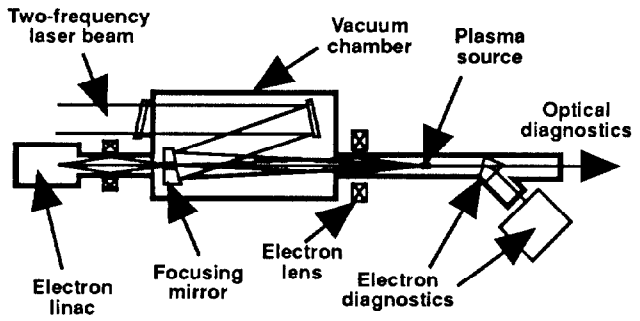

Figure 2: Cartoon overview of the main experimental apparatus.

small hole drilled in the large CO_2 laser focusing mirror, allowing the electrons and laser to propagate collinearly as is necessary for the experiment. The electrons are focused to a spot of about 260 μm diam which is smaller than the laser spot allowing good coupling of the electrons to the plasma wave. A double-focusing sector magnet selects the energy of the accelerated electrons which are detected by the electron diagnostics. These will be discussed in more detail in a later section.

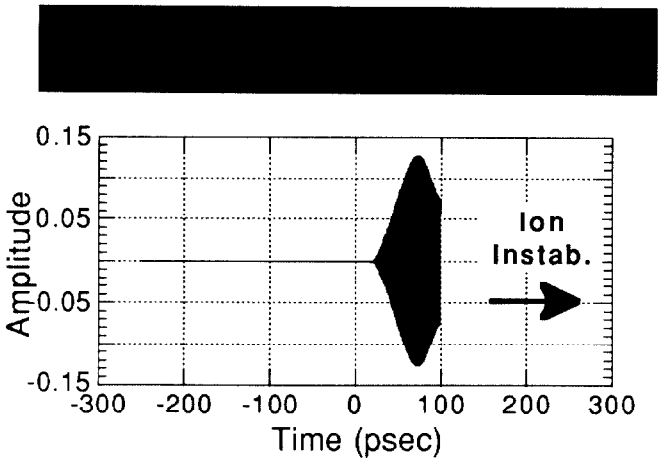

Figure 3: Bottom graph shows a calculation of the plasma wave amplitude vs. time for our laser parameters and the laser rising at t=0 psec. The model cannot predict what happens later in time due to ion instabilities. The top image is an actual streak of Cherenkov light from the linac electrons with the same time scale as the graph.

MODELING OF THE EXPERIMENT

With the laser parameters listed in Table 1, one can model the experiment[8] to find out what sort of dynamics to expect in the experiment. For example, the plasma formation can be modeled using the proven tunneling ionization theory[9] and the

Table 1: Experimental parameters for the laser, plasma, plasma wave, and electron injector.

Laser	
Source	CO_2 laser
Wavelengths	10.591, 10.289μm
Energy per line (typ.)	60 J, 15 J
Spot radius w_o	150 μm
Rayleigh range $2z_o$	1.3 cm
Electron quiver vel.	0.17, 0.07
Pulse risetime	150 psec
Pulse FWHM	300 psec
Plasma	
Source	Tunnel ionization
Density	8.6×10^{15} cm^{-3}
Gas	Hydrogen
Plasma period ν_p^{-1}	1.2 psec
Plasma wave wavelength	360 μm
Lorentz factor γ_{ph}	34
Accel. gradient for 11% wave	1 GeV/m
Electrons	
Source	RF LINAC
Energy	2 MeV
Peak current	200 mA
Emittance	6π mm-mrad
Focused spot radius	130 μm
RF frequency	9.3 GHz
Micropulse separation	107 psec
Electrons per micropulse	1.7×10^7
Micropulse length	10 psec

time-dependent density one thereby calculates can be inserted into a computation of the plasma wave growth. The result of such a modeling is shown in Fig. 3. The plasma reaches full ionization at best focus after about 25 psec into the 150 psec rise of the laser pulse. At this point, the plasma wave begins to grow until relativistic saturation occurs after about 70 psec. This particular calculation was for $\omega_{pe} = \Delta\omega$. If one sets ω_{pe} slightly *above* $\Delta\omega$, the relativistic saturation is delayed and a peak wave amplitude of 40% can be expected.[10]

The timing of the CO_2 laser and the 1 nsec FWHM linac macropulse is set to within ±100 psec. However, due to the technique by which the CO_2 pulse is generated, it is not possible to phase the exact *micropulse* timing to the timing of the peak fields in the plasma wave. A typical streak of the electrons (from Cherenkov light) is shown in the image above the graph in Fig. 3. One can see that there will be roughly a 50% probability that a micropulse will interact with a field of at least half the maximum fields of the plasma wave. The probability of interacting with higher and higher fields continues to drop until there is an approximately 10% chance of a micropulse interacting with the peak plasma wave fields.

DETAILED EXPERIMENTAL SETUP

A more detailed view of the experimental setup is shown in Fig. 4. The CO_2 laser and the electrons are both focused into

the plasma which is located at the center of a cross piece in the vacuum chamber. The back- and forward-scattered CO_2 light as well as the Thomson scattered probe beam are indicated by arrows. These three scattering diagnostics comprise the optical diagnostics of the wave amplitude mentioned earlier.

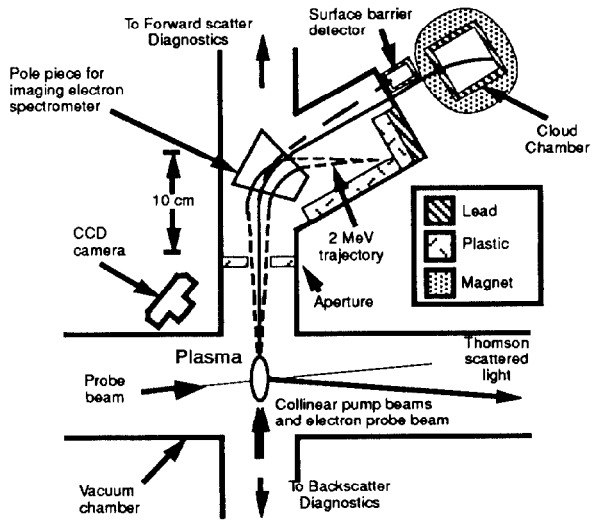

Figure 4: Detailed view of the experimental setup.

Injected electrons which do not interact with the plasma wave follow a small-radius trajectory and are dumped in a plastic beam dump as shown in Fig. 4. Electrons which are accelerated follow a larger radius trajectory and are detected in one of the electron diagnostics: a silicon surface barrier detector (SBD) or a diffusion cloud chamber.

The SBD, along with a preamplifier, produces a signal of about 20 mV per electron and can thus easily detect single electrons. It also has the advantage of providing a quantitative measurement of the number of electrons over a large dynamic range (by changing the preamplifier gain). But it has one major disadvantage and that is its sensitivity to x-rays. In fact, one cannot discern the difference between an electron signal and an x-ray signal except through the statistics of many data shots and null tests. For the experimental setup shown in Fig. 4, the contribution from x-ray noise varies from about 30 electrons worth of signal when the electron spectrometer is set to 3.5 MeV down to < 1 electron worth of signal when the spectrometer is set to 20 MeV.

The other electron detector is a simple, home-made diffusion cloud chamber[11] which uses a methanol bath at dry ice temperature in a chamber of 1 ATM of dry air. A piece of felt wicks the methanol up to the top of the chamber and the methanol vapor falls back into the bath, going through a region of supersaturation. The electrons ionize the air and the methanol condenses on the ions along the electrons' path. The chamber is shielded in lead and surrounded by a coil which can be energized to provide a ≈ 260 G vertical magnetic field throughout the active region of the cloud chamber. The tracks are recorded by frame-grabbing CCD camera. The big advantage of the cloud chamber aver the SBD is that it is essentially immune to x-ray noise. Although x-rays do produce some ionization of the gas and thus visible tracks, the tracks are typically short and kinked as they are due to low energy (<50 keV) electrons which are kicked out by the x-ray absorption in the dry air. The actual signal due to accelerated electrons should appear quite distinct from these tracks. They should be straight tracks, traversing the entire field of view of the camera and they should appear to originate form the aperture in the chamber.

EXPERIMENTAL RESULTS

Null tests

Ideally, the presence of signals on the two electron detectors should only occur if the three main components of the experiment are present. These are; (1) the plasma, (2) the injected electrons, and (3) the beat wave. If any of these are turned off, we would expect that there would be no signal on the electron detectors unless some other physics is occurring besides beat wave acceleration. The result of these null tests are summarized in Table 2. As indicated in the third column, we see no evidence of acceleration by the laser beam itself, of acceleration of non-injected electrons (from for example, instability-heated electrons), or of spontaneous generation of an accelerating structure through some mechanism other than beat wave (as in, for example, Raman forward scattering).

Cloud chamber data

When the plasma, external electron source, and two-frequency laser are fired up simultaneously in about 140 mT of hydrogen gas, tracks are observed in the cloud chamber as seen in Fig. 5. For the image in Fig. 5(a), the electron spectrometer was set to direct 5.2 MeV electrons into the aperture of the cloud chamber and the magnetic field surrounding the cloud chamber was off. The tracks have the characteristics of high-energy electrons discussed earlier; that is, straight lines, long range, and directionality. The scatter in the angles is probably dominated by scatter in the 25 μm Mylar vacuum-exit window and the ≈ 6 cm of 1 ATM air between the vacuum window and the beginning of the field of view. Subsequent calibrations indicate that Fig. 5(a) is

Table 2: Summary of the key null tests performed.

Condition	Result	Conclusion
Linac & 2-frequency laser but no plasma (chamber evacuated).	Only usual* x-ray noise.	No acceleration by laser only.
2-frequency laser & plasma but no linac (linac beam blocked).	No signal at all‡.	No trapping of background plasma electrons or SRS-generated tail.
Single-line laser & linac & plasma (no second frequency).	Only usual* x-ray noise.	No substantial level of stimulated Raman forward scattering.

* Usual x-ray noise ≈ 10 electrons worth of signal.
‡ No signal => less than 1 electrons worth of signal.

composed of about 10^3 tracks.[12] For Fig. 5(b), the external magnetic field was energized causing the electron trajectories and therefore the tracks to bend. For this shot, the electron spectrometer was again set to 5.2 MeV as in Fig. 5(a). An image with a small number of tracks was chosen in order to see individual tracks. Three theoretical trajectories calculated for 5.2 MeV electrons are overlaid onto this image. The good agreement indicates that the electrons were within 10% of 5 MeV; i.e., 2.5 times higher energy than the injection energy of 2 MeV.

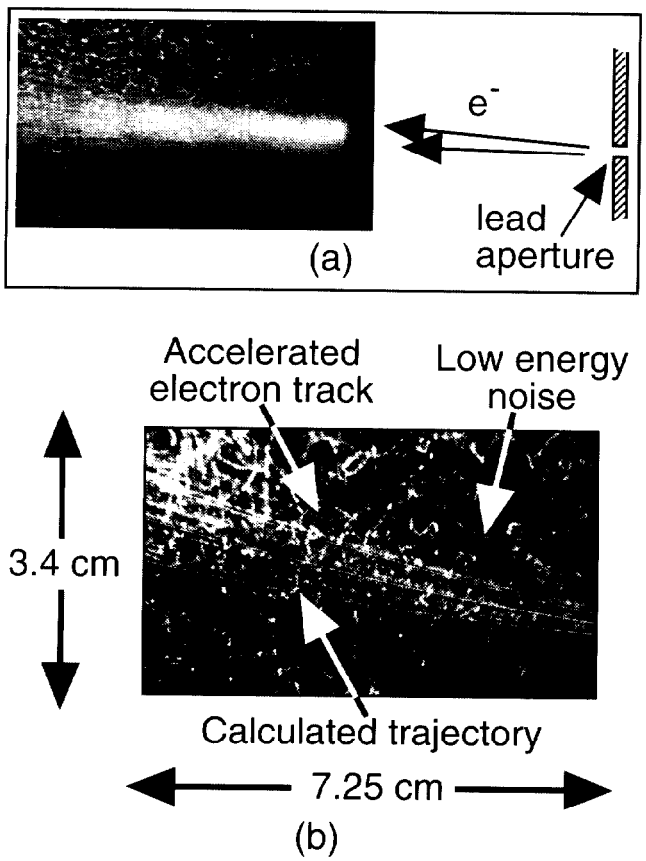

Figure 5: Images of tracks in cloud chamber with the electron spectrometer set to send 5.2 MeV electrons into the aperture of the cloud chamber. (a) No external magnetic field. Relative location of the aperture is shown. (b) With 260 G external field. Calculated trajectories are overlaid as the thin white curves.

Surface barrier detector data

While the cloud chamber dramatically confirms the existence of accelerated electrons, it is not a very quantitative diagnostic. The SBD, however, is quantitative since the signal level is directly proportional to the number of electrons striking the silicon detector. Figure 6 shows the SBD signal vs. fill pressure of H_2 gas in the vacuum chamber for a variety of electron spectrometer settings. Since we expect that the gas is fully ionized and since the beatwave is a resonant phenomena, we can predict the range of pressures over which a substantial level of plasma wave will exist. This is shown by the hatched bar along the pressure axis near 135 mT. Experimentally, we find that we must overfill the chamber by about 8% or so. This is probably due to hydrodynamic expansion of the plasma column during the ≈100 psec time scale of the interaction. The individual points on Fig. 6 are single laser shots. All the shots which show electrons signals above the x-ray noise (which is around 200–300 mV) also show evidence for a large-amplitude plasma wave on the three optical diagnostics.[8] Shots with small electron signals

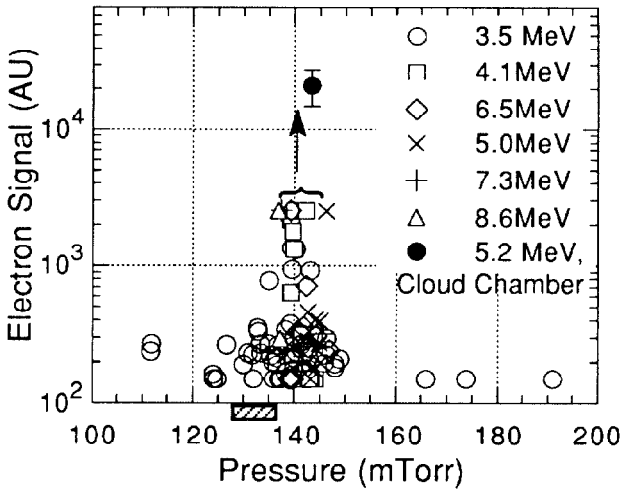

Figure 6: SBD signal vs. vacuum-chamber fill pressure for various settings of the electron spectrometer. The open points are from Detector A and the solid point is from a calibration of the intensity of the tracks in Fig. 5(a). The hatched bar is the range of the expected resonance.

near 140 mT either did not have a plasma wave (according to the optical diagnostics) due to lack of two frequencies in the laser or they did have a plasma wave but the electrons were unsynchronized due to the micropulse structure of the linac beam. The data in Fig. 6 were taken with the experimental arrangement of Fig. 4 and for this arrangement, the SBD detector is referred to Detector A.

Detector A is limited to viewing energies below 9 MeV due to the maximum field obtainable in the electrons spectrometer. To extend the electron energy measurements to energies beyond 9 MeV, a new port was added to the electron spectrometer at about 5× the radius of curvature shown by the long-dashed curve in Fig. 4. In this case, two SBD's were collecting data for each shot: Detector B at the low energy position and Detector C at the high energy position. A summary of the number of detected electrons (SBD signal in mV times electrons/mV sensitivity of the detector/preamp combination, corrected for any limiting lead apertures placed over the detectors) vs. the energy location of the detectors. Although this data was accumulated over many laser shots, we can see that the numbers are falling off rapidly with energy, going out to 20 MeV. This rapid fall-off with energy can be expected for two reasons. First, the electrons are not pre-bunched and therefore occupy all phases in the acceleration buckets. Secondly, energy-bunching is expected to occur only for longer acceleration lengths where transient or start-up phase

slippage is not important. In this experiment, however, the electrons execute a large swing in phase as they accelerate from $\gamma = 5$ (well below the Lorentz factor for the wave, γ_{ph}) to $\gamma \approx 20$ (slightly above γ_{ph}).

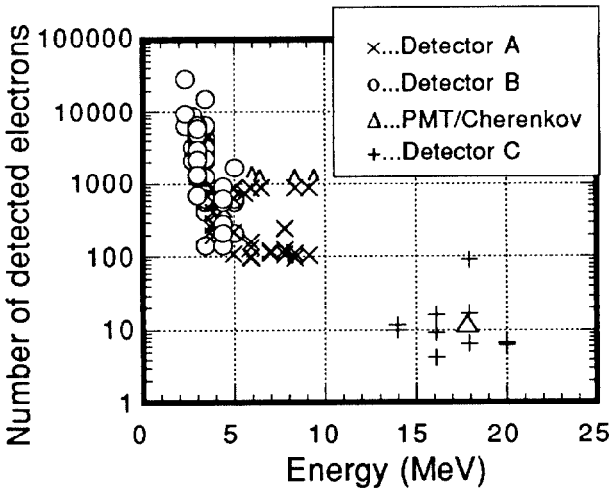

Figure 7: Number of detected electrons vs. energy location of the detectors. Data is from many shots. Detectors B and C were on-line together. Triangle point is from a gaseous Cherenkov tube coupled to a photomultiplier.

The maximum energy seen in these shots was 20 MeV. This is an energy gain of 18 MeV over the nominal 1 cm of interaction length which corresponds to an average accelerating gradient of 1.8 GeV/m. From the engineering formula given in the introduction, this corresponds to a wave amplitude of $\varepsilon \approx 20\%$. This is within a factor of two of the best one would expect for our experimental parameters. The maximum energy gain may be limited by the dynamics discussed in connection with Fig. 6.

CONCLUSION

To summarize, the acceleration of an externally injected beam of electrons in a relativistic electron plasma wave has been demonstrated. Acceleration is only observed when the linac injector, the two-frequency laser, and the plasma are all on simultaneously. The numbers of accelerated electrons is correlated with independent optical diagnostics. Energies out to 20 MeV have been observed implying an average gradient (over $\approx$ 1 cm) of about 1.8 GeV/m, only about 2 times lower than the optimum expected for our experimental parameters.

To conclude, it appears that the plasma beat wave accelerator concept can be relied upon to provide energy gains nearly in accordance with theory. If one chooses a different parameter space--for example, replacing the CO_2 laser with a two-frequency laser operating at a wavelengths around 1 μm--one can find theoretical energy gains of several hundred MeV from gradients approximately 10× higher than demonstrated in this experiment.[8] Such an experiment would essentially be an extension of the current CO_2 laser experiment in that it requires no new physics. Thus, with today's glass laser technology, one could envision building a small plasma accelerator based on the beat wave concept which would approach the GeV energy range.

ACKNOWLEDGMENTS

The authors would like to acknowledge useful discussions with Drs. W. B. Mori and P. Mora, and Professors J. M. Dawson, T. Katsouleas, and R. Williams and thank D. Gordon for his technical assistance. This work is supported by the U. S. Department of Energy under grant no. DE-FG03-92ER40727.

REFERENCES

1. C. E. Clayton, K. A. Marsh, A. Dyson, M. Everett, A. Lal, W. P. Leemans, R. Williams, and C. Joshi, "Ultrahigh-gradient acceleration of injected electrons by laser-excited relativistic electron plasma waves", Phys. Rev. Lett. 70, 37 (1993).
2. See, for example, *Advanced Accelerator Concepts*, ed. by C. Joshi, AIP Conf. Proc. No. 193 (Amer. Inst. Phys., New York, 1989).
3. See, for example, the Special Issue on Plasma-Based High Energy Accelerators, IEEE Trans. Plasma Sc., PS-15, (1987) and C. Joshi, W. B. Mori, T. Katsouleas, J. M. Dawson, J. M. Kindel, and D. W. Forslund, "Ultrahigh gradient particle acceleration by intense laser-driven plasma density waves", Nature 311, 525 (1984).
4. M. Rosenbluth and C. S. Liu, "Excitation of plasma waves by two laser beams", Phys. Rev. Lett. 29, 701, (1972).
5. C. E. Clayton, K. A. Marsh, W. P. Leemans, M. Everett, and C. Joshi, "A terawatt, short-pulse, multiline CO_2 laser facility based on optical free-induction decay" (to be published).
6. W. P. Leemans, C. E. Clayton, W. B. Mori, K. A. Marsh, A. Dyson, and C. Joshi, "Plasma physics aspects of tunnel-ionized gases", Phys. Rev. Lett. 68, 321 (1992) and W. P. Leemans, C. E. Clayton, W. B. Mori, K. A. Marsh, P. K. Kaw, A. Dyson and C. Joshi, "Experiments and simulations of tunnel-ionized plasmas", Phys. Rev. A 46, 1091 (1992).
7. C. E. Clayton and K. A. Marsh, "A 2 MeV, 100 mA electron accelerator for a small laboratory environment", Rev. Sci. Instr., 64, 728 (1993) and C. E. Clayton and K. A. Marsh, "A versatile 2 MeV, 200 mA compact x-band linac", (this proceedings).
8. C. Joshi, C. E. Clayton, K. A. Marsh, A. Dyson, M. Everett, A. Lal, W. P. Leemans, R. Williams, T. Katsouleas, and W. B. Mori, "Acceleration of injected electrons by the plasma beat wave accelerator", in AIP Proceedings of Workshop on Advanced Accelerator Concepts, Port Jefferson, Ed. J. Wurtele, to be published (1992).
9. P. B. Corkum, N. H. Burnett and F. Brunel, "Above-threshold ionization in the long-wavelength limit," Phys. Rev. Lett., vol. 62, pp. 1259-62, March 1989.
10. C. M. Tang, P. Sprangle, and R. N. Sudan, "Dynamics of space-charge waves in the laser beat wave accelerator", Phys. Fluids 28, 1974 (1985).
11. A. Langsdorf, Jr., "A continuously sensitive diffusion cloud chamber", Rev. Sci. Inst. 10, 91 (1939).
12. C. E. Clayton, K. A. Marsh, A. Dyson, M. Everett, A. Lal, W. P. Leemans, R. Williams, and C. Joshi, "Experimental Demonstration of Laser Acceleration of Electrons via Relativistic Plasma Waves", Proc. of the SPIE OE-LASE '93 Conf., Jan. 16-23, 1993, Los Angeles, CA.